Liquid crystal droplet array for non-contact electro-optic inspections

2010 J. Phys. D: Appl. Phys. 43 365103

(http://iopscience.iop.org/0022-3727/43/36/365103)

IOP PUBLISHING JOURNAL OF PHYSICS D: APPLIED PHYSICS

J. Phys. D: Appl. Phys. **43** (2010) 365103 (5pp) doi:10.1088/0022-3727/43/36/365103

Liquid crystal droplet array for non-contact electro-optic inspections

Hongwen Ren[1], **Haiqing Xianyu**[2] **and Shin-Tson Wu**[2]

[1] Department of Polymer-Nano Science and Engineering, Chonbuk National University, Jeonju, Chonbuk 561-756, South Korea

[2] College of Optics and Photonics, University of Central Florida, Orlando, FL 32816, USA

E-mail: hongwen@jbnu.ac.kr

Received 7 June 2010, in final form 5 August 2010
Published 25 August 2010
Online at stacks.iop.org/JPhysD/43/365103

Abstract

We report a high density liquid crystal (LC) droplet array for non-contact inspection. The incident light is modulated by changing the shape of each droplet using a dielectric force even though the electrode and droplet array are separated by a fairly large air gap. The reshaped LC droplets cause colour change which is easily inspected by the human eye. In a sample with 30 μm thick polymer cavity and 130 μm air gap, LC droplet surface reshaping is clearly observed as the applied voltage exceeds 40 V_{rms}. Potential application of such a LC droplet array for inspecting the defected thin-film-transistor pixels is emphasized.

(Some figures in this article are in colour only in the electronic version)

1. Introduction

Thin-film-transistor liquid crystal displays (TFT-LCDs) have been widely used for mobile phones, computer screens, TVs and data projectors. To improve fabrication yield, inspecting and repairing malfunctioned TFT pixels are necessary before cell sealing. Various inspection methods have been proposed [1–7], but most of them are unnoticeable to human visual perception due to low contrast or using the method of indirectly touching the pixel surface [4]. Because the indirect touching method still uses spacers to control the gap between the detector and the TFT electrode, the pixels may be damaged by the spacers. Therefore, a non-contact method is preferred, in which the electrode is separated from the surface of the employed liquid crystal (LC) medium by an air gap.

The conventional testing system for a non-contacting light modulator is shown in figure 1. From bottom to top are the electrode, air gap, dielectric mirror, modulator, electrode, imaging objective and CCD camera. When a light is incident to the modulator, the changed intensity can be detected by the CCD camera and data analysed by the image processor [4]. The modulator is the key part of the testing system. Owing to the unique electro-optical property, liquid crystalline materials have been used in various optical modulators [8–12]. In figure 1 if a pure LC is used as the modulator, then the dielectric mirror is needed in order to sustain a homogeneous

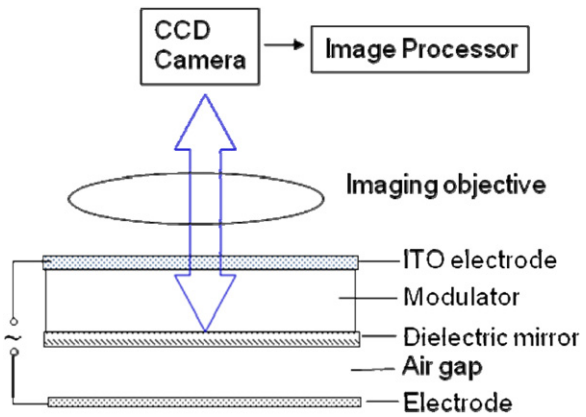

Figure 1. Schematic non-contact testing system using a light modulator.

LC layer and prevent LC from flowing. Due to the existence of dielectric mirror and air gap, the modulator will require a very high operating voltage. Let us consider the following example: an LC cell is composed of 3 μm homogeneous LC layer (Merck BL-038, $\Delta\varepsilon = 16.4$, $\varepsilon_{\parallel} = 21.7$) and 50 μm air gap. When a voltage $V = 100\,V_{rms}$ is applied to the cell, only 1 V drops across the LC layer, which is smaller than the threshold voltage (~1.88 V) of the LC media. Therefore, the LC will not be reoriented even though the dielectric mirror is not considered. If a polymer-dispersed liquid crystal (PDLC)

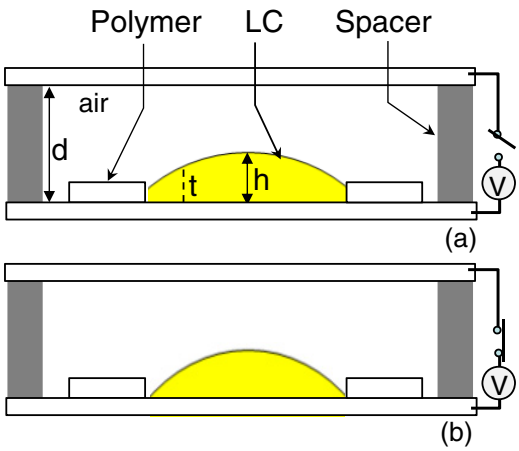

Figure 2. Side-view structure of a LC droplet–air gap cell (*a*) without voltage and (*b*) in voltage-on state.

film is employed as modulator, then the dielectric mirror may be removed because PDLC is solid and can adhere to the top electrode surface. However, in comparison with a LC modulator, PDLC usually requires a much higher operating voltage due to the strong anchoring force of polymer cavity surfaces [8]. The operating voltage will dramatically increase if a thin air gap exists above the PDLC layer. It is a big challenge to develop a non-contact LC modulator with a fairly large air gap in which LC can still be reoriented by a fairly low voltage.

In this paper, we report the use of a high-density LC droplet array for the optical modulator. The droplets modulate light mainly based on their shape change. The reshaped droplets cause LC reorientation, thus leading to colour shift due to the change in effective birefringence. Although a fairly large air gap exists in the cell, the required operating voltage keeps fairly low. Such a LC droplet array is particularly attractive for inspecting the defects of TFT-LCD panels.

2. Device structure and basic theory

Figure 2 depicts the side-view structure of the LC modulator. A tiny LC droplet is fixed on one electrode surface and surrounded by a polymer wall. Another electrode is placed above the droplet with an air gap to form a cell. These two electrodes are placed in parallel position and controlled by a spacer (such as the Mylar film). The cell gap d is larger than the apex distance h of the droplet. The droplet surface is very smooth due to surface tension. Without an external voltage, as figure 2(*a*) shows, the droplet surface is in the relaxing state (maximal curvature without an external force to change its shape). At a given voltage V, the LC droplet experiences an electric field which can be expressed as [13]

$$E_t = \frac{V}{t + ((d-t)\varepsilon_{\mathrm{LC}}/\varepsilon_{\mathrm{air}})}, \tag{1}$$

where t is the height of the droplet from the electrode surface to the curved surface of the droplet along the vertical direction and $\varepsilon_{\mathrm{LC}}$ denotes the effective dielectric constant of the LC and $\varepsilon_{\mathrm{air}}$ ($\sim$1) represents the dielectric constant of air.

From equation (1), at the droplet centre the electric field is expressed as

$$E_{\mathrm{centre}} = \frac{V}{h + (d-h)\varepsilon_{\mathrm{LC}}}, \tag{2}$$

and at the droplet border the electric field is

$$E_{\mathrm{border}} = \frac{V}{t_{\mathrm{b}} + (d-t_{\mathrm{b}})\varepsilon_{\mathrm{LC}}}, \tag{3}$$

where t_{b} is the height of the droplet border. In comparison with equations (2) and (3), we find that $E_{\mathrm{centre}} > E_{\mathrm{border}}$. Because the surface of the LC droplet is smoothly curved, the electric field across the droplet surface has a gradient distribution. According to dielectrophoretic theory, when an ac voltage is present the LC droplet bears a dielectric force [14]:

$$F_{\mathrm{DEP}} = 2\pi R^3 \varepsilon_{\mathrm{air}} Re\left(\frac{\varepsilon_{\mathrm{LC}} - \varepsilon_{\mathrm{air}}}{\varepsilon_{\mathrm{air}} + 2\varepsilon_{\mathrm{LC}}}\right)\nabla E^2, \tag{4}$$

where R is the radius of a LC droplet and E denotes the electric field on the curved droplet surface. This dielectric force causes LC molecules to shift towards the high electric field region. This dielectrophoretic effect is similar to that of the patterned electrode technique [15]. As a result, the surface of the droplet will shrink in order to get a new balance between the surface tension force and the dielectric force, as illustrated in figure 2(*b*). The reshaped profile will alter the phase retardation of the probing beam, leading to a colour change when observed between crossed polarizers.

3. Device fabrication

To fabricate a cell, as figure 2 shows, first we prepared a polymer cavity array using our previously reported method [16]. A UV curable monomer NOA65 (Norland Optical Adhesive) was spread on an indium tin oxide (ITO)-coated glass substrate using a blade. After coating, the film was placed in horizontal position for several minutes to achieve uniform thickness. It was then exposed to UV light ($\sim$30 mW cm^{-2}) through a photomask for 20 s. The uncured monomer was removed by ethanol. Figure 3(*a*) shows the patterned polymer cavity array observed under a polarized optical microscope (POM) in transmissive mode. The holes represent the areas without monomer. The surface of each hole in the array presents an octagon shape and the diameter of the cavity aperture is $\sim$50 μm. The distance of the adjacent holes is $\sim$8 μm. The thickness of the film was measured to be $\sim$30 μm by observing its cross-section using the POM.

Here we chose BL-038 (Merck; its nematic phase is from $-$20 to 100 °C) as the LC material. The LC was mixed with a solvent (dichloromethane) at $\sim$10 wt%. The solvent helps to decrease the LC surface tension and dilute the LC concentration in the mixture. When a small amount of the mixture was dripped on the patterned film surface, the solvent was then evaporated by heating. After thorough evaporation, LC formed droplets in the polymer cavities. Figure 3(*b*) shows the formed LC droplets observed using POM. Two polarizers are used, so that a star pattern for each LC droplet could be

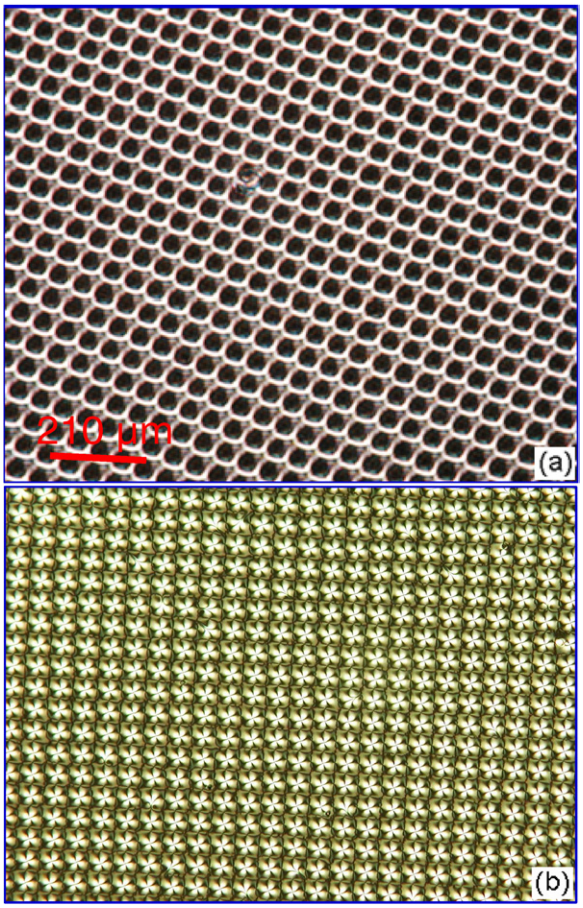

Figure 3. (*a*) The polymer cavity array observed through a transmissive POM and (*b*) the LC droplet array observed after filling the cavities.

observed. The size of droplets is uniform. The dome shape of the droplets can be inferred from their imaging properties. We typed a letter 'A' on a piece of transparency foil to serve as object. By adjusting the distance between droplets and object, an inverted image array was observed, implying that the LC droplet bears convex shape. The aperture ratio of the film can be estimated as follows: LC occupation area/(LC occupation area + non-LC covering area). From figure 3(*b*), the aperture ratio is estimated to be ∼80%.

4. Results and discussion

To study the impact of voltage on the LC droplets, we placed another ITO glass plate above the LC droplet array. The gap of the two glass plates was controlled to be ∼160 μm using two striped Mylar films. The cell, whose structure is shown in figure 2, was observed using a POM between crossed polarizers with a high magnification. Each droplet can be clearly observed with greenish colour in the central area, as figure 4(*a*) shows. When a 100 V_{rms} voltage was applied across the ITO electrodes, the observed colour changed to bluish, as shown in figure 4(*b*). Such a result indicates that the LC droplets respond to the external voltage although the air gap is as large as ∼130 μm.

As for the boundary condition, we magnified the droplet array in the $V = 0$ state and focused on the surface of several droplets, as shown in figure 4(*c*). There are some disclination lines across the droplets. The centre droplet is almost connected to its adjacent droplets. Each droplet is also surrounded by four dark regions. The dark regions are the polymer area without or with less LC on its surface. Because of these regions, each LC droplet is almost isolated. The aperture of each droplet is not perfectly round due to the relatively low surface tension of the LC (<20 dynes cm^{-1}). From the droplet centre to its border, light intensity decreases gradually which means the dome of the droplet presents spherical-like shape.

Because the size of each droplet is too small, we measured its electro-optic property in a dark room. The cell was placed in the vertical direction and a collimated He–Ne laser was used as probing beam at normal incidence. The beam passing through a LC droplet was expanded by an imaging lens and received by a photodiode detector. A diaphragm was placed in front of the detector. At $V = 0$, the detector had maximum intensity. When a voltage was applied to the cell, the surface of the droplet was reshaped, thus a portion of the laser beam was blocked by the diaphragm. Figure 5 is a plot of voltage-dependent light intensity. At low voltage, the air gap shields most of the voltage. As a result, the LC droplet cannot be activated by the dielectric force. As $V > 40\ V_{rms}$, the intensity starts to decrease because the generated dielectric force takes effect. As the voltage keeps increasing, the intensity decreases gradually. At $V = 100\ V_{rms}$, the intensity change is quite noticeable. Such a result is consistent with the observed colour shift shown in figure 4.

A response time is an important factor for light modulation, especially when it is intended for probing the defects of millions of TFT pixels on a large substrate. To measure the response time, we still used the same experimental setup except for displaying the detected optical signals in a digital oscilloscope. Figure 6 shows the measured intensity change (upper curve) with time when a 100 V pulse amplitude was applied to the electrodes. The rise and decay times were measured to be ∼52 ms and ∼50 ms, respectively. The measured intensity was noisy because of the employed oscilloscope as well as the increased background light. However, the cyclic response (two periods given) shows that the LC droplets return to their original state very well.

In comparison with the results shown in figure 4, we also studied the dynamic response of some much smaller droplets. These tiny droplets were formed near the cell border where less mixture filled in the polymer cavities. Through POM, the small droplets did not give observable colour change when they were activated at 100 V_{rms}. Due to the small size each droplet was totally trapped in its cavity. From equations (2) and (3), t_b is close to h. Therefore, the gradient of electric field is decreased significantly and the droplet cannot be reshaped easily. Such a result also implies that LC reorientation is mainly due to the shape change in the droplet.

From our results, LC droplets can be reshaped by an external voltage although the air gap is as large as ∼130 μm. Such a droplet array is useful as an optical modulator for inspecting the defects in TFT pixels, where non-contact inspection is preferred. The TFT arrays take the place of the top ITO substrate in this case (shown in figure 2). A typical TFT

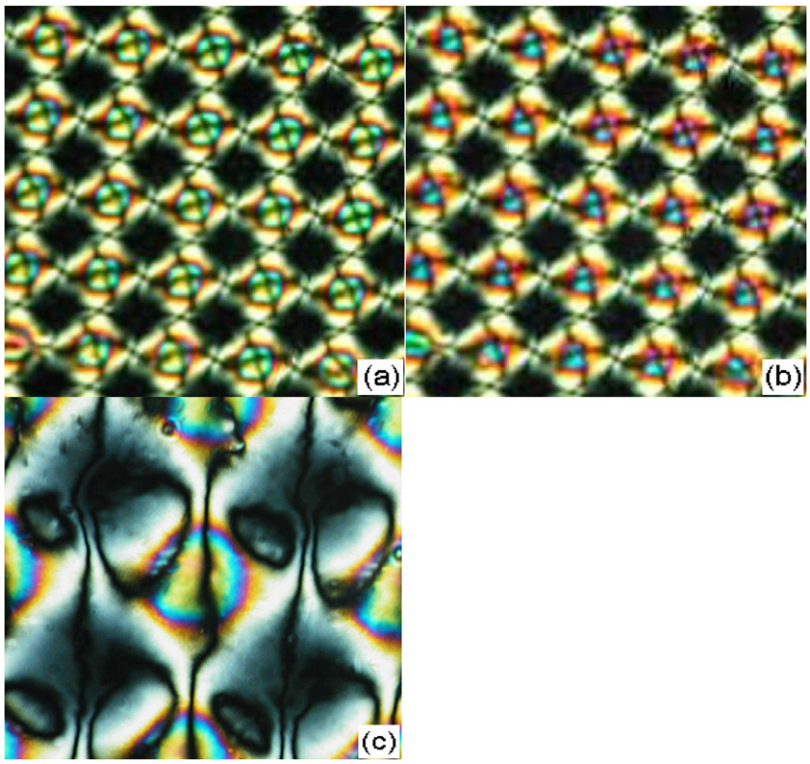

Figure 4. The observed colour with different voltages applied to the cell. (*a*) $V = 0$, (*b*) 100 V, and (*c*) $V = 0$ with a large magnification.

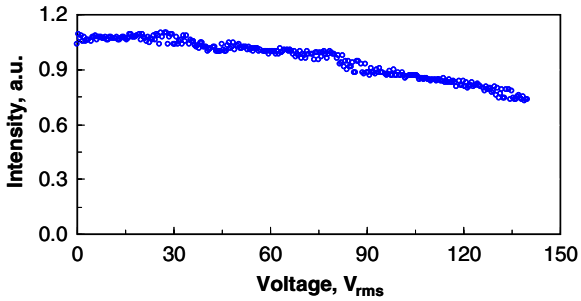

Figure 5. Measured voltage-dependent light intensity change.

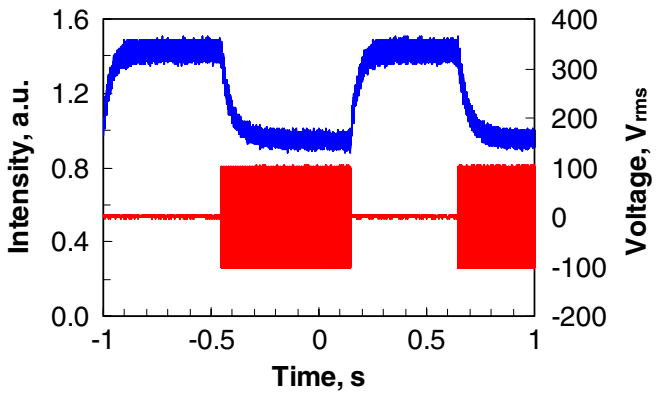

Figure 6. Measured response time of a LC droplet with two cycle periods.

pixel size is ∼300 μm × 100 μm; it covers about ten 50 μm LC droplets. The functionality of the TFT pixel can be inspected by the colour change in the corresponding LC droplets when the pixel is turned on or off. To improve precision, we can further increase the LC droplet density so that each TFT pixel will cover more LC droplets.

From equations (2) and (3), the gradient of the electric field is dependent on the geometric structure of the droplet and the dielectric constant of LC material. It is possible to enhance the electric field gradient by optimizing the droplet shape and choosing LC with a suitable ε_{LC}. Under such conditions, the required operating voltage can be kept low even for a reasonably large air gap. Although the top surface of the LC droplets is sustained by air, each droplet in its cavity is very stable and will not flow out when the cell is placed in the vertical direction or shaken severely. The reason is that the gravity force is negligible for tiny droplets [17, 18]. Instead, the surface tension force and the adhesion force play the main roles to anchor the droplets and sustain the droplets with spherical shape.

5. Conclusion

We demonstrated a non-contact optical modulator using a high density LC droplet array with a large air gap. The LC droplets can modulate light based on dielectrophoresis. For the modulator with ∼130 μm air gap, LC droplets can still be activated with a relatively low voltage (40 V_{rms}). A higher voltage applied to the droplets can cause an obvious light intensity change and a significant colour shift. The rise and decay time is each ∼50 ms. Such a LC droplet array is preferred for designing non-contact inspection devices. One

potential application of the LC droplet array is to inspect the defected TFT pixels.

Acknowledgments

H Ren is indebted to the support by research funds of the Chonbuk National University and the UCF group is partially supported by the AFOSR under Contract No FA95550-09-1-0170.

References

[1] Wisnieff R L, Jenkins L, Polastre R J and Troutman R R 1990 *SID Symp. Digest* **21** 190–3
[2] Hiroi T, Maeda S, Kubota H, Watanabe K and Nakagawa Y 1994 *Proc. 2nd IEEE Workshop on Applications of Computer Vision (Sarasota, FL)* (Los Alamitos, CA: IEEE Computer Society) pp 26–34
[3] Maeda S, Ono M, Kubota H and Nakatani M 1999 *Syst. Comput. Japan* **30** 72–84
[4] Son J S, Lee J H and Lee S H 2006 *Curr. Appl. Phys.* **6** 84–90
[5] Lu C-J and Tsai D-M 2005 Automatic defect inspection for LCDs using singular value decomposition *Int. J. Adv. Manuf. Technol.* **25** 53–61
[6] Lee C H, Jeong C, Chang M and Park P 2008 Implementation of TFT inspection system using the common unified device architecture (CUDA) on modern graphic hardware *10th Int. Conf. on Control, Automation, Robotics and Vision (Hanoi, Vietnam)* pp1899–902
[7] Liu Y-H, Wang C-K, Yu Ting, Lin W-Zh, Kang Zh-H, Chen Ch-Sh and Hwang J-Sh 2009 *Int. J. Mol. Sci.* **10** 4498–514
[8] Drzaic P 1995 *Liquid Crystal Dispersions* (Singapore: World Scientific)
[9] Bunning T J, Natarajan L V, Tondiglia V P and Sutherland R L 2000 *Annu. Rev. Mater. Sci.* **30** 83–115
[10] Vardanyan K K , Qi J, Eakin J N, De Sarkar M and Crawford G P 2002 *Appl. Phys. Lett.* **81** 4736–8
[11] Rudhardt D, Fernandez-Nieves A, Link D R and Weitz D A 2003 *Appl. Phys. Lett.* **82** 2610–12
[12] Lu S Y and Chien L C 2007 *Appl. Phys. Lett.* **91** 131119
[13] Ren H, Xianyu H, Xu S and Wu S T 2008 *Opt. Express* **16** 14954–60
[14] Pohl H A 1978 *Dielectrophoresis* (Cambridge: Cambridge University Press)
[15] Kim Y, Francl J, Taheri B and West J L 1998 *Appl. Phys. Lett.* **72** 2253–5
[16] Ren H, Ren D and Wu S T 2009 *Opt. Express* **17** 24183–8
[17] Vafaei S and Podowski M Z 2005 *Nucl. Eng. Des.* **235** 1293–301
[18] Ren H, Xu S and Wu S T 2010 *Opt. Commun.* **283** 3255–8